

Supplementary Material for: Rationalizing Steroid Interactions with Lipid Membranes: Conformations, Partitioning, and Kinetics

Kalina Atkovska,[†] Johannes Klingler,[‡] Johannes Oberwinkler,[¶] Sandro
Keller,[§] and Jochen S. Hub^{*,||,⊥}

[†]*Institute for Microbiology and Genetics and Goettingen Center for Molecular Biosciences,
37077 University of Goettingen, Göttingen, Germany*

[‡]*Molecular Biophysics, Technische Universität Kaiserslautern (TUK), Kaiserslautern, Germany*

[¶]*Institut für Physiologie und Pathophysiologie, Philipps-Universität Marburg, 35037 Marburg,
Germany*

[§]*Molecular Biophysics, Technische Universität Kaiserslautern (TUK), 67663 Kaiserslautern,
Germany*

^{||}*Institute for Microbiology and Genetics and Goettingen Center for Molecular Biosciences,
University of Goettingen, 37077 Göttingen, Germany*

[⊥]*Theoretical Physics, Saarland University, 66123 Saarbrücken, Germany*

E-mail: jochen.hub@physik.uni-saarland.de

Methods

Safety Statement

No unexpected or unusually high safety hazards were encountered.

Force Field Parameters

The Slipids force field¹⁻³ was used for POPC, and water was described with the TIP3P water model.⁴ The parameters of all steroids were derived using the Antechamber module⁵ from the AmberTools 14 package. The general Amber force field (GAFF)⁶ atom types with RESP charges were used. Here, geometry optimization and calculation of the electrostatic potential was performed with Gaussian 09,⁷ while the RESP charge fit was performed by Antechamber. The topology files were created by the tleap module in AmberTools, and converted into Gromacs format by ACPYPE.⁸ For cholesterol, we repeated the calculations with both, Slipids and GAFF parameters.

Derivation of Partial Atomic Charges. Consistent with common GAFF parameterizations, we used HF/6-31G* (HF/6-31+G* for the anionic steroids) level of theory for the electrostatic potential (ESP) calculations, which were performed in vacuum. However, the free energies of partitioning calculated using these parameters showed in some cases significant deviations from the experimentally measured values. Namely, the calculated values were in most cases more negative than the experimental ones, suggesting the force field description of the steroids was insufficiently polar. To test this, we recalculated the ESP surfaces in water, using the polarizable continuum model (PCM) with default settings as implemented in Gaussian 09. Indeed, using the partial charges derived from these calculations, the calculated $\Delta G_{\text{part}}^{\circ}$ values increased by $\sim 6 \text{ kJ mol}^{-1}$ on average. Finally, we assumed a linear relationship between the magnitude of the charges and $\Delta G_{\text{part}}^{\circ}$, and we derived “optimal” partial charges as a linear combination of the vacuum-derived and water-derived charges, in order to achieve best possible agreement to experiment. According to the weights of the water-derived and vacuum-derived charges needed to achieve the opti-

mal charges, we found that most of the studied steroids belong to two groups: 1) weight of the water-derived charges of 1, and 2) weights of the water- and vacuum-derived charges of ~ 0.4 and ~ 0.6 respectively. Using the optimal charges, we achieved excellent agreement between the calculated and experimental free energies of partitioning (Fig. 6). Exceptions include few relatively polar steroids that lay mainly horizontally in the membrane (estriol, hydrocortisone, ethinylestradiol), for which even the water-derived charges were insufficiently polar. The rest of the steroids for which experimental free energy of partitioning was not available were classified in one of the abovementioned groups, based on chemical similarity, and the respective weights for the water-derived and vacuum-derived charges were used to calculate the optimal charges. In summary, vacuum-derived charges were used for β -sitosterol, cholesterol, dehydroergosterol, and pregnonolone sulfate; water-derived charges were used for aldosterone, β -estradiol, hydrocortisone, corticosterone, dexamethasone, ethinylestradiol, estriol, fludrocortisone acetate, pregnenolone, and tetrahydrodeoxycorticosterone; while for the rest of the steroids a combination of vacuum- and water-derived charges was used. Gromacs topologies with the optimal charges can be downloaded from <https://biophys.uni-saarland.de/steroids.html>. For the sake of completeness, topologies with the original vacuum-derived partial charges are also provided.

Equilibrium Simulations Setup

The simulations setup was identical for all systems. Lipid bilayers containing 242 POPC (1-palmitoyl-2-oleoyl-*sn*-glycero-3-phosphocholine) molecules, 14 steroid molecules (5.5mol%), and 35 water molecules per lipid were created using the MemGen web server (<http://memgen.uni-goettingen.de>).⁹ Systems containing charged steroids were neutralized with 14 Na counterions. First, the potential energy of the systems was minimized within 100 steps using the steepest descent algorithm. In order to prevent any bias in the steroid orientation and position in the membrane from the membrane building procedure, using simulated annealing the systems were slowly heated to 370 K within 15 ns, simulated at 370 K for 50 ns, and then cooled down to 300 K within

15 ns and equilibrated for another 20 ns at 300 K. Then, production runs of 500 ns were performed at 300 K.

The MD simulations were performed with the Gromacs 5 simulation software.¹⁰ Bonds and angles in the water molecules were constrained using the SETTLE algorithm,¹¹ and the rest of the bonds in the system were constrained with the LINCS algorithm.¹² An integration step of 2 fs was used. Short-range repulsive and attractive dispersion interactions were described together by a Lennard-Jones (LJ) potential, which was cut off at 1.4 nm. Electrostatics were treated with the particle-mesh Ewald scheme^{13,14} using a grid spacing of 0.12 nm and a real-space cut-off of 1.0 nm. In the production runs, the temperature was controlled at 300 K using velocity rescaling¹⁵ ($\tau = 0.5$ ps), and using separate coupling for membrane and solvent. The pressure was controlled at 1 bar by a semi-isotropic coupling to a Berendsen barostat¹⁶ ($\tau = 2$ ps), whereby scaling in the xy -plane (membrane plane) was independent from the scaling in the z -direction. Dispersion correction for the energy and pressure was applied.

For the tilt and depth analysis, C-3 and C-17 atoms from the steroid core were defined as “head” and “tail” atoms respectively, corresponding to the vertical orientation of cholesterol in the membrane. The tilt of the steroid in the membrane was given as the cosine of the angle α between the steroid “axis” and the z -axis (normal to the membrane). The steroid axis was defined as the line connecting the head and tail atoms. The depth of the head and tail atoms in the membrane was computed as the vertical distance (Δz) between each atom and the centre of mass of the bilayer. Both quantities ($\cos \alpha$ and Δz) were extracted from each frame of a 500 ns simulation, and the averages and standard deviations over all 26 steroid molecules are shown in Figs. 3 and 5. The distributions of both quantities for each steroid are given in Supplementary Figs. S1 and S2. The lines showing the approximate positions of the phosphate, choline, and ester groups in Fig. 5 with respect to the membrane centre of mass represent averages over all phosphorus, nitrogen, and ester oxygen atoms respectively, from all POPC molecules in the bilayers, over the same simulation frames taken as for the rest of the analyses, over all simulations.

ITC Measurements

The partitioning between water and POPC bilayers of androstenedione, cortisone, dihydrotestosterone, hydrocortisone, prednisone, dehydroepiandrosterone, dehydroepiandrosterone sulfate, pregnenolone, pregnenolone sulfate, and progesterone, was studied by isothermal titration calorimetry (ITC).¹⁷ To this end, suspensions of large unilamellar vesicles composed of POPC were titrated to a steroid solution. Lipid concentrations in the ITC injection syringe were between 20 and 100 mM, and steroid concentrations in the ITC sample cell were 50 μM . Measurements were performed at 22° C, 27° C, and 37° C. The buffer used was 10 mM 4-(2-hydroxyethyl)-1-piperazineethanesulfonic acid (HEPES) with 145 mM NaCl, 2 mM CaCl_2 , 2 mM MgCl_2 , and 0.5% (v/v) dimethyl sulfoxide (DMSO). In order to obtain 50 μM solutions, steroids were dissolved in pure DMSO at a concentration of 10 mM and diluted 200-fold into DMSO-free buffer.

Raw thermograms from ITC measurements were integrated with NITPIC.¹⁸ Isotherms obtained by integration were analyzed¹⁹ in terms of a partitioning model based on a mole-ratio partition coefficient, K_0 .²⁰ Besides K_0 , the standard molar enthalpy of partitioning, $\Delta H_{\text{part}}^{\circ \text{exp}}$, was directly obtained from the analysis. 95% confidence intervals (CIs) were calculated for K_0 and $\Delta H_{\text{part}}^{\circ \text{exp}}$ ²¹ and then estimated for $\Delta G_{\text{part}}^{\circ \text{exp}}$ and $-T\Delta S_{\text{part}}^{\circ \text{exp}}$ via propagation of uncertainty.

In an ITC titration with vesicles, the steroids initially have access to only one leaflet of the bilayer (the “outside” of the vesicles). Thus, the amount of lipid they can interact with depends on their ability to translocate across the bilayer on experimental timescales (here: minutes). This is quantified by the lipid accessibility factor, γ , which is 0.5 or 1 for negligible or rapid membrane translocation on experimental timescales, respectively.²² In this work, we did not estimate γ for each steroid but instead used $\gamma = 0.5$ throughout.

Charged steroids (dehydroepiandrosterone sulfate and pregnenolone sulfate), were analyzed in terms of a surface partitioning model where Coulombic effects were accounted for by Gouy–Chapman theory.^{22,23} Here, the contribution to the membrane surface charge density by a membrane-associated molecule is quantified by its effective charge, z_e , which is usually equal to or smaller than its nominal charge, z . For our analysis, we fixed z_e at z . For compatibility with the partition-

ing data from the simulations, we calculated the apparent partition coefficients K_{app} , based on K_0 and z_e for a molar fraction of steroid in the bilayer of 5.9%.

The experimental $\Delta G_{\text{part}}^{\circ \text{exp}}$ values shown in Figs. 6 and 7 correspond to 27°C for 4-androstenedione, cortisone, dihydrotestosterone, hydrocortisone, and prednisone, and to 22°C for dehydroepiandrosterone, dehydroepiandrosterone sulfate, pregnenolone, pregnenolone sulfate, and progesterone. Full data from the ITC measurements are shown in the Supplementary table S1.

The partition coefficients from refs. 24–27 were converted as necessary to mole-ratio partition coefficients K_0 . For consistency, the accessibility factor γ was taken to be 0.5, resulting in correction of the $\Delta G_{\text{part}}^{\circ \text{exp}}$ value by $RT \ln 0.5 = -1.7 \text{ kJ mol}^{-1}$.

Simulation-Based Calculations of POPC/Water Partition Coefficients

To calculate the free energies of transfer of the steroid molecules from bulk water solution into a POPC bilayer, we first calculated a potential of mean force (PMF) $\mathcal{W}(z)$ for permeation of each solute across such a bilayer, using the umbrella sampling method.^{28,29} The umbrella sampling simulations were conducted similar to previous work.^{30,31} Starting structures were taken from randomly chosen snapshots from an equilibrium simulation of a membrane patch containing 32 POPC molecules and 65 water molecules per lipid. The mass-weighted centre of mass (COM) position of the steroid along the membrane normal, z_m , was taken as reaction coordinate for solute permeation where $z_m = 0$ corresponds to the COM of the membrane. The membrane COM was computed from a weighted sum over the lipid atoms within a cylinder that was centred at the respective solute and aligned along the z axis. Here, the cylinder was defined by a radius of 1.5 nm and a continuous switching function in radial direction, as implemented in Gromacs 2016. The umbrella windows were separated by $\Delta z_{\text{win}} = 0.4 \text{ \AA}$. To save computational resources, multiple umbrella windows were sampled in one MD simulation, which has only a marginal effect on the PMFs.³⁰ Here, we kept a distance of $\Delta Z_{\text{sol}} = 1.7 - 2.5 \text{ nm}$ along z between neighboring solutes, depending on the size of the solute. Hence, to collect all umbrella histograms, $N_{\text{sim}} = \Delta Z_{\text{sol}} / \Delta z_{\text{win}}$ simulations were set up for each steroid. The solutes were inserted at the umbrella centres, and overlapping water

molecules were removed. Overlaps between the solute and lipid atoms were removed by gradually switching on LJ interactions between the solute and the rest of the system within 15000 simulation steps. During these insertion simulations only, a large virtual site atom was added to the centre of the steroid rings to enforce that lipid tails are quickly repelled from the ring. The energy of each structure was subsequently minimized. The umbrella sampling simulations were carried out for 50 ns each, using a harmonic umbrella potential acting on the COM of the solute with force constant of $2000 \text{ kJ mol}^{-1} \text{ nm}^2$. The temperature was set to 300 K through a stochastic dynamics integrator ($\tau = 0.1 \text{ ps}$).³² The pressure was controlled at 1 bar using semiisotropic coupling to the Berendsen barostat, as in all other simulations ($\tau = 1 \text{ ps}$). In order to save computational resources, LJ interactions were cut off at 1.0 nm, since we have previously found that PMF calculations for lipid membrane permeation are relatively insensitive to the LJ cut-off down to 0.8–0.9 nm.³⁰ All other simulation parameters were the same as in the equilibrium simulations.

Constructions of PMFs. After removing the first 10 ns for equilibration, the PMFs were computed with the weighted histogram analysis method (WHAM),³³ as implemented in the gmx wham software.³⁴ The integrated autocorrelation times (IACTs) of the umbrella windows were incorporated in the WHAM iteration procedure as described by Kumar et al.³³ IACTs were estimated as described in reference 34, and smoothed along z using a Gaussian filter with $\sigma = 0.2 \text{ nm}$. First, non-periodic and non-symmetrized PMFs were computed. These PMFs were reasonably symmetric with respect to the membrane centre and exhibited only a small offset between the two bulk water regimes, suggesting that the PMFs were reasonably converged. Subsequently, a periodic PMF was computed and symmetrized with respect to the membrane centre ($z = 0$). Statistical uncertainties of the PMFs were calculated using the Bayesian bootstrap of complete histograms.³⁴

Calculation of $\Delta G_{\text{part}}^{\circ \text{ sim}}$ from the PMFs. By definition, the mole-ratio partition coefficient K_0 is equal to

$$K_0 = \frac{c_{i,\text{memb}}/c_{\text{POPC,memb}}}{c_{i,\text{bulk}}}, \quad (1)$$

where $c_{i,\text{memb}}$ and $c_{i,\text{bulk}}$ are the molar concentrations of the steroid in the membrane and bulk solution respectively, while $c_{\text{POPC,memb}}$ is the molar concentrations of POPC in the membrane. To

evaluate $c_{i,\text{memb}}/c_{i,\text{bulk}}$, we used (i) that the PMF $\mathcal{W}(z)$ was defined to zero on bulk water, and (ii) that the steroid concentration is proportional to $\exp(-\mathcal{W}(z)/k_bT)$, where k_b is the Boltzmann constant and T the temperature. Then, $c_{i,\text{memb}}/c_{i,\text{bulk}}$ is obtained by integrating the steroid concentration along z in the membrane with thickness d , and in a bulk region of the same volume:

$$\frac{c_{i,\text{memb}}}{c_{i,\text{bulk}}} = \frac{\int_{-d/2}^{d/2} e^{-\mathcal{W}(z)/k_bT} dz}{\int_{-d/2}^{d/2} dz} = \frac{1}{d} \int_{-d/2}^{d/2} e^{-\mathcal{W}(z)/k_bT} dz \quad (2)$$

The concentration of POPC lipids in the membrane is $c_{\text{POPC,memb}} = 2/(d * A_L)$, where $A_L = 0.65 \text{ nm}^2$ is the area per lipid of POPC. Hence, we obtain for the partition coefficient

$$K_0 = \frac{1}{2} A_L \int_{-d/2}^{d/2} e^{-\mathcal{W}(z)/k_bT} dz. \quad (3)$$

For the partition free energy, we use

$$\Delta G_{\text{part}}^{\circ \text{sim}} = -RT \ln(K_0 c_{\text{water,bulk}}), \quad (4)$$

where $c_{\text{water,bulk}} = 55.5 \text{ mol dm}^{-3}$ denotes the bulk water concentration. The uncertainty of $\Delta G_{\text{part}}^{\circ \text{sim}}$ was computed from the uncertainty of the PMFs using standard error propagation.

Simulation-Based Calculations of the Cyclohexane/Water Partition Coefficients

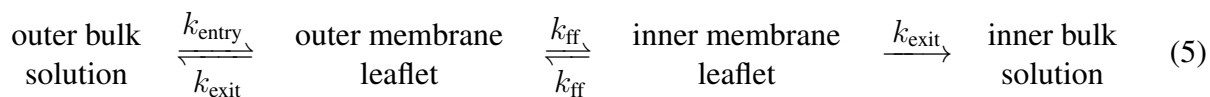
The water/cyclohexane partition free energies for steroids were computed from the difference between the solvation free energies in water and in cyclohexane. The solvation free energies into water and cyclohexane were calculated using discrete thermodynamic integration (TI) along an alchemical reaction coordinate λ , where $\lambda = 0$ corresponds to the non-interacting state, and $\lambda = 1$ corresponds to the fully interacting state. Here, TI was conducted in two separate steps. First, LJ interactions between the steroid and solvent were turned on with zero partial charges on the steroid

atoms. Second, Coulomb interactions between the steroid and solvent were turned on at full LJ interactions. The TI for turning on LJ interactions were conducted using the following 24 λ -points: 0, 0.05, 0.1, 0.125, 0.15, 0.175, 0.2, 0.225, 0.25, 0.3, 0.35, 0.4, 0.45, 0.5, 0.55, 0.6, 0.65, 0.7, 0.75, 0.8, 0.85, 0.9, 0.95, and 1. The TI for turning on Coulomb interactions were conducted using 12 λ -points, which were evenly distributed between 0 and 1.

The TI simulations were set up by inserting a steroid molecule into a box of 1378 water molecules, or into a box of 178 cyclohexane molecules. Solvent atoms that overlapped with the steroid were removed. Cyclohexane was modelled with the GAFF⁶ topology taken from <http://virtualchemistry.org>,³⁵ and water was modelled with the TIP3P model.⁴ After minimizing the energy, each system was simulated for 5 ns for each λ -point. The temperature was controlled at 300 K using a stochastic dynamics integrator ($\tau = 0.3$ ps), and the pressure was controlled at 1 bar with an isotropic Berendsen barostat ($\tau = 1$ ps). All other parameters were identical to the lipid membrane simulations. After removing the first 100 ps for equilibration, $\langle \partial H / \partial \lambda \rangle$ was computed from the average over each trajectory, where H is the Hamiltonian, and the uncertainty was computed using binning analysis. The change in free energy $\Delta G_{\text{TI}} = \int_0^1 \langle \partial H / \partial \lambda \rangle d\lambda$ was computed with the trapezium rule, and the uncertainty of ΔG_{TI} with standard error propagation. The total solvation free energies for the steroid in water and cyclohexane were taken as the sums of the ΔG_{TI} 's for the respective LJ and Coulomb interactions. Again, uncertainties for total solvation free energy and the partition free energy were computed with error propagation.

Probability for Membrane Permeation per Binding Event

The probability for a steroid permeation event per binding event was computed with the following reaction scheme:



Here, k_{ff} denotes the flip–flop rate, k_{exit} the rate for exiting the membrane, and k_{in} the rate for entering the membrane from the outer bulk. We assume (a) a symmetric membrane, hence the flip–flop and exiting rates do not depend on the direction of the transitions; and (b) a sink in inner bulk region, that is, molecules reaching the inner bulk are taken out of the system. The following rate equations describe the system:

$$\frac{dC_o}{dt} = -(k_{\text{exit}} + k_{\text{ff}})C_o + k_{\text{ff}}C_i + k_{\text{entry}}C_{\text{bulk}} \quad (6)$$

$$\frac{dC_i}{dt} = k_{\text{ff}}C_o - (k_{\text{exit}} + k_{\text{ff}})C_i \quad (7)$$

Here, C_o , C_i , and C_{bulk} denote the concentration in the outer leaflet, inner leaflet, and outer bulk, respectively. We consider the steady state of the system, $dC_o/dt = dC_i/dt = 0$. In steady state, Eqs. 6 and 7 yield

$$k_{\text{exit}}C_o + k_{\text{exit}}C_i = k_{\text{entry}}C_{\text{bulk}} \quad (8)$$

suggesting that for each molecule exiting the membrane (either towards the inner or towards the outer bulk region, left-hand side of Eq. 8) a molecule is added to the outer leaflet from the outer bulk reservoir (right-hand side of Eq. 8). In addition, Eqs. 6 and 7 yield

$$\frac{C_o}{C_i} = 1 + \frac{k_{\text{exit}}}{k_{\text{ff}}}. \quad (9)$$

The probability for a permeation event, that is an exit from the inner leaflet, per binding event is

$$P_{\text{perm}} = \frac{k_{\text{exit}}C_i}{k_{\text{entry}}C_{\text{bulk}}} = \left(\frac{k_{\text{exit}}}{k_{\text{ff}}} + 2 \right)^{-1}. \quad (10)$$

The limiting cases of Eq. 10 are as expected. For $k_{\text{exit}} \gg k_{\text{ff}}$, we have $P_{\text{perm}} \approx 0$ because most molecules exit before the first flip–flop event occurs. For $k_{\text{exit}} \ll k_{\text{ff}}$, we have $P_{\text{perm}} \approx 1/2$ because the molecule may equilibrate between the two leaflets before exiting the membrane. With $k_{\text{exit}} = k_{\text{ff}}$, we obtain $P_{\text{perm}} = 1/3$ because (a) exit or flip–flop occur with probability 1/2, and

(b) permeation requires an odd number of flip–flop events plus one exit event, that is overall an even number of events with probability of $1/2$ each. Summing up all even powers of $1/2$ yields $\sum_{i=1}^{\infty} (1/2)^{2i} = 1/3$, in agreement with Eq. 10 for the case $k_{\text{exit}} = k_{\text{ff}}$.

Challenges with Computing the Flip–Flop Barrier

To estimate the rates of steroid flip–flop, we computed the position-dependent diffusion coefficient along the membrane normal and the PMF for flip–flop transitions. Accurate calculations of flip–flop free-energy barriers are complicated by the fact that the centre of mass (COM) position of the steroid relative to the membrane COM is not always a good reaction coordinate for flip flop transitions. When using a poor reaction coordinate, however, the flip–flop barrier may be partially integrated out, leading to an overestimate of the flip–flop rate. Hence, to compute the flip–flop barrier for cholesterol, Bennett *et al.* defined the reaction coordinate for flip–flop from the position of the hydroxyl group of cholesterol,³⁶ whereas other groups computed two-dimensional PMFs as a function of COM position and orientation of the steroid, from which they obtained the minimum free-energy path.^{37,38} For steroids with multiple polar groups, however, computing the barrier for flip–flop is further challenged by the fact that, upon pulling the steroid into the membrane, it may drag water into the hydrophobic membrane core, thereby forming a partial aqueous defect connecting the steroid with the head groups of one leaflet. Such partial aqueous defects have been identified as a source for sampling problems and integrated out barriers, also referred to as “hidden barriers”.³⁹ To the best of our knowledge, there is no general solution for such problems, except for computationally expensive methods such as the string method for optimizing the minimum free-energy path.⁴⁰ However, visual inspection of the simulations provides a hint whether the PMF may be affected by integrated out barriers due to partial aqueous defects: if the steroid becomes fully dehydrated in the membrane core, such artefacts are probably minor. By contrast, if the steroid forms partial aqueous defects, the barrier may be underestimated. In this work, we observed that steroids with zero or one hydroxyl group become fully dehydrated at the membrane core, suggesting that the flip–flop barriers are correct. For steroids with two or three hydroxyl groups, however,

we occasionally observed such partial aqueous defects, suggesting that the flip–flop barrier may be underestimated. Hence, the flip–flop rates for steroids with two or three hydroxyl groups reported here should be taken as an upper bound of the true flip–flop rate. The qualitative trends, however, namely the strongly decreasing flip–flop rates with increasing number of hydroxyl groups (Fig.8), are correct.

Calculation of Flip–Flop and Exit Rates

In this study, guided by the work by Bennett *et al.*,³⁶ we used a reaction coordinate that mainly quantifies the position of the polar steroid atoms with respect to the membranes centre, and we obtained a second set of PMFs, denoted $\mathcal{W}_q(z)$. We defined the COM weighted by the absolute value of the atomic partial charge, $\mathbf{R}_q = \sum_i |q_i| \mathbf{r}_i / \sum_i |q_i|$, where q_i and \mathbf{r}_i denote the partial charge and the Cartesian coordinates of atom i , and the sum is taken over all atoms of the steroid. Then, the reaction coordinate was defined as the position of \mathbf{R}_q relative to the mass-weighted COM of the membrane and projected onto the membrane normal (z -axis). For steroids that carry substitutions of similar polarity at their two ends, \mathbf{R}_q resembles the regular mass-weighted COM; in contrast, for highly asymmetric steroids whose substitutions at the C-3 and C-17 atoms strongly differ in polarity, \mathbf{R}_q is shifted towards the polar end, thereby mitigating the problem with integrated out flip–flop barriers. Indeed, for such asymmetric steroids such as β -sitosterol, cholesterol, and prednisone, the flip–flop barrier increased by up to 9 kJ/mol as compared to the barrier based on a mass-weighted COM definition. For each steroid, the flip–flop rate was computed from the PMF ($\mathcal{W}_q(z)$ or $\mathcal{W}(z)$) that exhibited the higher barrier for flip–flop.

The position-dependent diffusion coefficient $D(z)$ of the steroids along the membrane normal z was computed following Hummer, $D(z) = \text{var}(z) / \tau_z$, where $\text{var}(z)$ and τ_z denote the variance and the autocorrelation time of the z , respectively, as taken from the umbrella windows.⁴¹ Here, τ_z was computed by integrating the autocorrelation function of z , $C_z(t)$. To avoid that random modulations of $C_z(t)$ at larger t influence the τ_z estimates, we integrated $C_z(t)$ up to the time where $C_z(t)$ dropped for the first time below 0.05. In cases where $C_z(t)$ did not drop below 0.05 up to

$t = 500$ ps, $C_z(t)$ was integrated up to $t = 500$ ps. Subsequently, we smoothed $D(z)$ with a Gaussian filter with a width of 0.1 nm. $D(z)$ exhibited only small variations within the membrane core in the range $-2 \text{ nm} < z < 2 \text{ nm}$. Averaged over the membrane, the diffusion coefficient took values between $2.3 \times 10^{-5} \text{ nm}^2 \text{ ps}^{-1}$ and $7.3 \times 10^{-5} \text{ nm}^2 \text{ ps}^{-1}$ for the different steroids, corresponding to friction coefficients $\gamma_f = k_b T / (Dm)$ between 0.1 and 0.3 ps^{-1} . Here m is the mass of the steroid. Our calculated diffusion coefficients are in good agreement with the transverse diffusion coefficients for different steroids obtained with quasi-elastic neutron scattering.⁴² In the temperature range between 20°C and 36°C, these authors found diffusion coefficients between $0.6 \times 10^{-5} \text{ nm}^2 \text{ ps}^{-1}$ and $3.1 \times 10^{-5} \text{ nm}^2 \text{ ps}^{-1}$ for cholesterol, lanosterol, and ergosterol in DPPC membranes with 40% steroid content, thus providing a more crowded environment with slightly reduced diffusion coefficients as compared to the case of a single steroid in a POPC membrane considered here.

The flip–flop rate was computed following Kramers’ theory,⁴³ as follows:

$$k_{\text{ff}} = \left(\frac{m\omega_A^2}{2\pi k_b T} \right)^{1/2} / \int_{-z_1}^{z_1} \frac{e^{-\beta(\mathcal{W}^*(z) - \mathcal{W}^*(z_1))}}{D(z)} dz. \quad (11)$$

Here, $\pm z_1$ is the position of the two minima of the PMF corresponding to the equilibrium positions of the steroid in the two leaflets (see Fig. 8), ω_A is the angular frequency in the minima, obtained by fitting a parabola to the minima of the PMFs, and $\beta = (RT)^{-1}$ is the inverse temperature. The PMF $\mathcal{W}^*(z)$ denotes either the PMF based on the normal mass-weighted COM definition, $\mathcal{W}(z)$, or based on the partial-charge-weighted COM definition, $\mathcal{W}_q(z)$, whichever exhibited the higher barrier for flip–flop. As a control, we computed k_{ff} also using the simplified Kramers result, $k'_{\text{ff}} = \omega_A \omega_B / (2\pi \gamma_f) \exp(-\beta \Delta \mathcal{W}^*)$, where ω_B is the angular frequency at the flip–flop barrier, and $\Delta \mathcal{W}^*$ is the barrier height. The value of k'_{ff} was very close to k_{ff} .

The exit rate for steroids was computed analogously to Eq. 11,

$$k_{\text{exit}} = \left(\frac{m\omega_A^2}{2\pi k_b T} \right)^{1/2} / \int_{z_1}^{z_b} \frac{e^{-\beta(\mathcal{W}(z) - \mathcal{W}(z_1))}}{D(z)} dz. \quad (12)$$

Here, the integration was conducted from the PMF minimum at z_1 up to a position where the

steroid had left the membrane $z_b \approx 3.5$ nm, and we used purely the PMF based on the mass-weighted COM definition, $\mathcal{W}(z)$.

Estimate for Membrane Entry Rate, k_{entry}

An order-of-magnitude estimate for the rate of membrane entry was obtained from a thickness of a water layer, L_w , across which the steroid diffuses before membrane entry. Assuming a simple 1D diffusion, the time scale at which the steroid travels a distance of L_w is estimated by $t_w = L_w^2/(2D_w)$. From typical radii of eukaryotic cells or diameters of blood capillaries, we estimate $L_w \approx 10$ μm . Under experimental conditions with planar membranes, unstirred layers are expected in the order of $L_w \approx 100$ μm .⁴⁴ For LUVs, unstirred layers are comparable to the vesicle radius.⁴⁵ Diffusion constants of steroids in water were reported as $D_w \approx 7 \times 10^{-6}$ cm^2/s .⁴⁶ These values translate into $k_{\text{entry}} = 14$ s^{-1} for the cellular environment, 0.14 s^{-1} for planar membranes, and $1.4 \cdot 10^5$ s^{-1} for LUVs with a radius of 0.1 μm . The value for the cellular environment is only a rough estimate, and it may be modulated by factors such as a possible small free-energy barrier for membrane entry (Fig. 8C, yellow curve, $z = \pm 2$ nm), the cell size, a complex membrane geometry, or crowding. Likewise, the value for vesicles strongly depends on the radius of the vesicle.

Notably, these k_{entry} estimates consider membrane entry after the initial expose of the system with the steroid, hence taking the initial diffusion of steroids to the membrane into account. For a system in equilibrium, a detailed balance criterium between steroids in the membrane and the bulk can be employed, leading to larger equilibrium entry rates as compared to k_{entry} .

Supplementary Figures and Tables

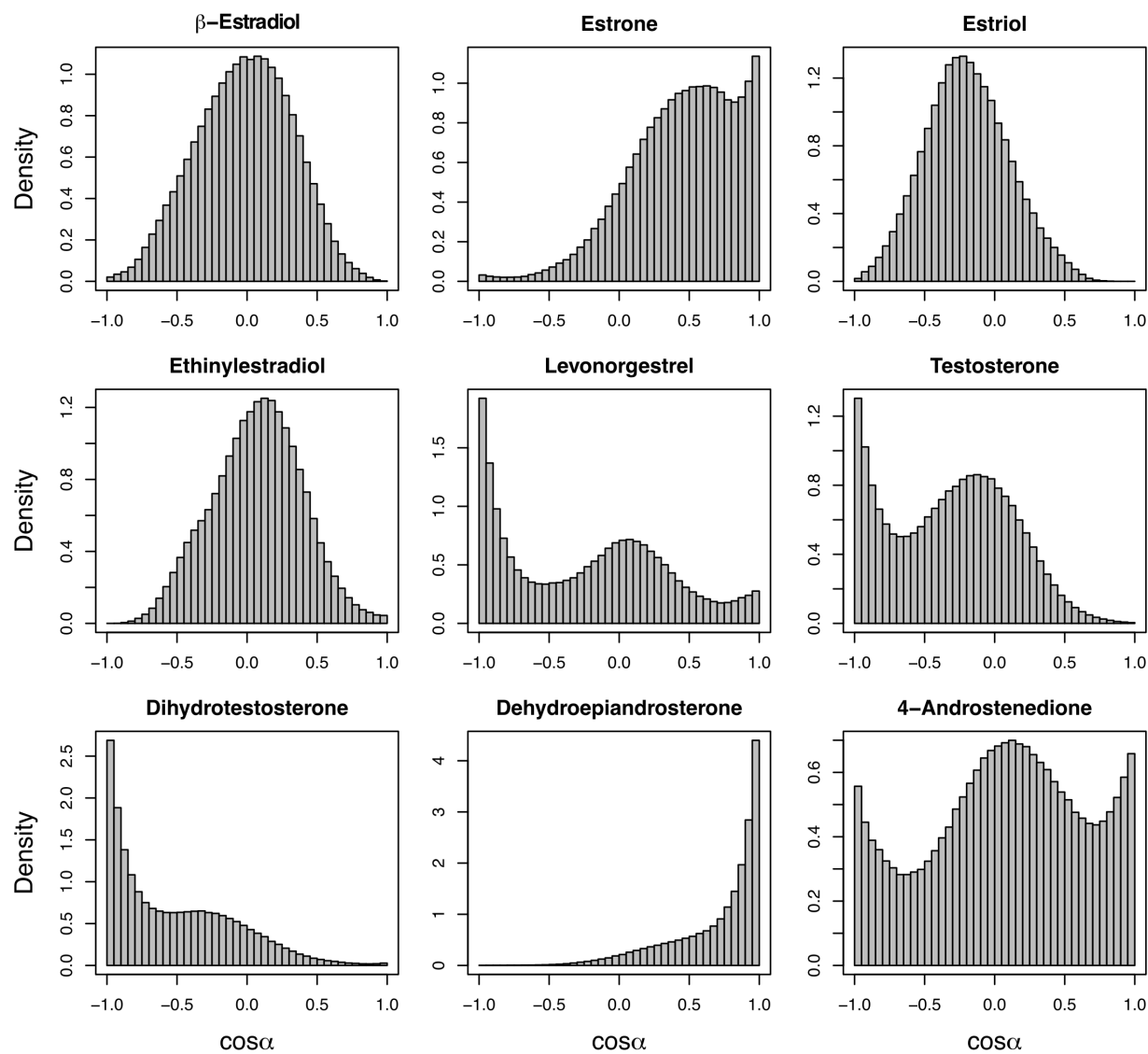


Figure S1: Distributions of the cosine of the tilting angle α of each steroid from 500 ns simulations.

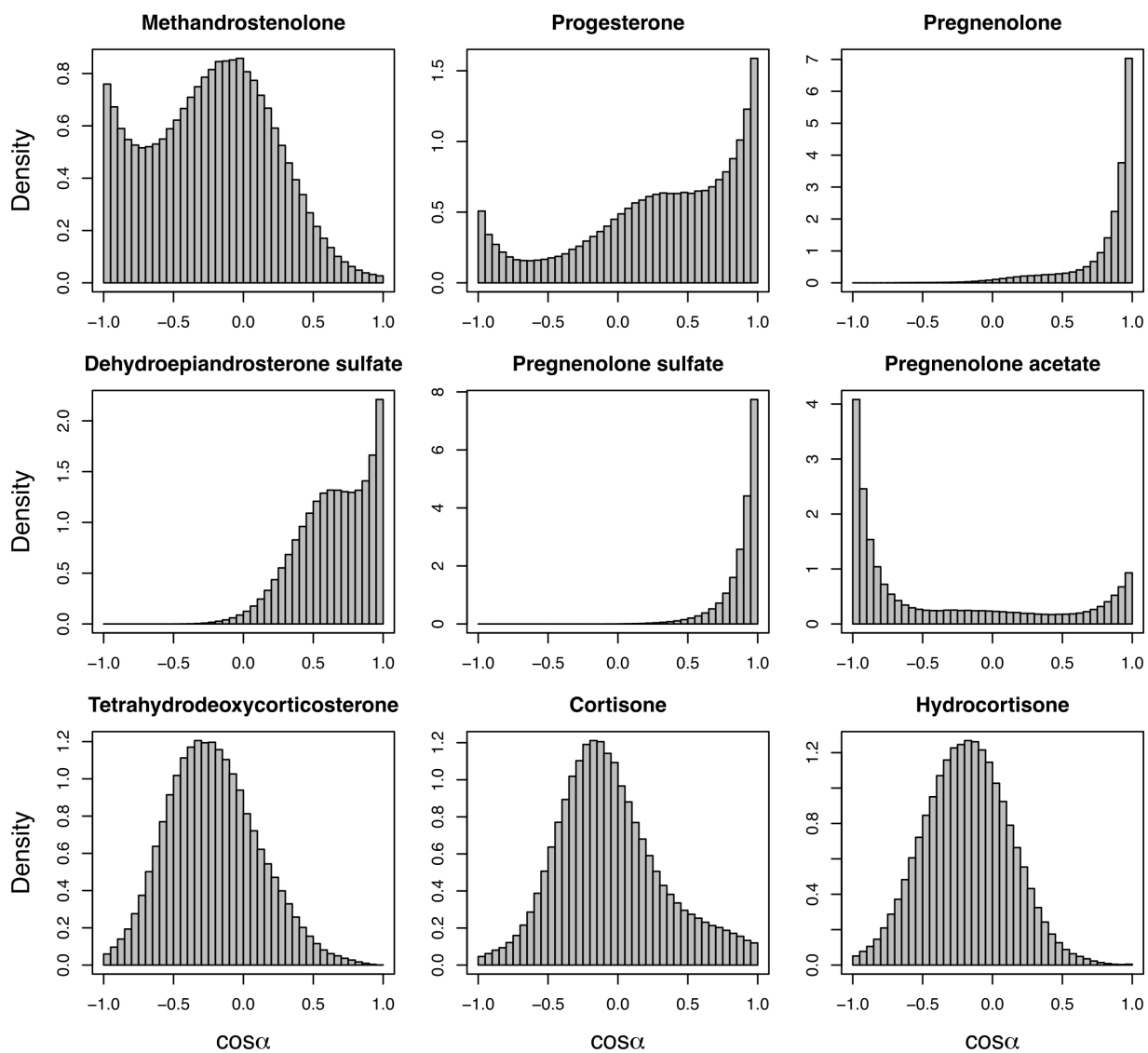


Figure S1 (Cont.): Distributions of the cosine of the tilting angle α of each steroid from 500 ns simulations.

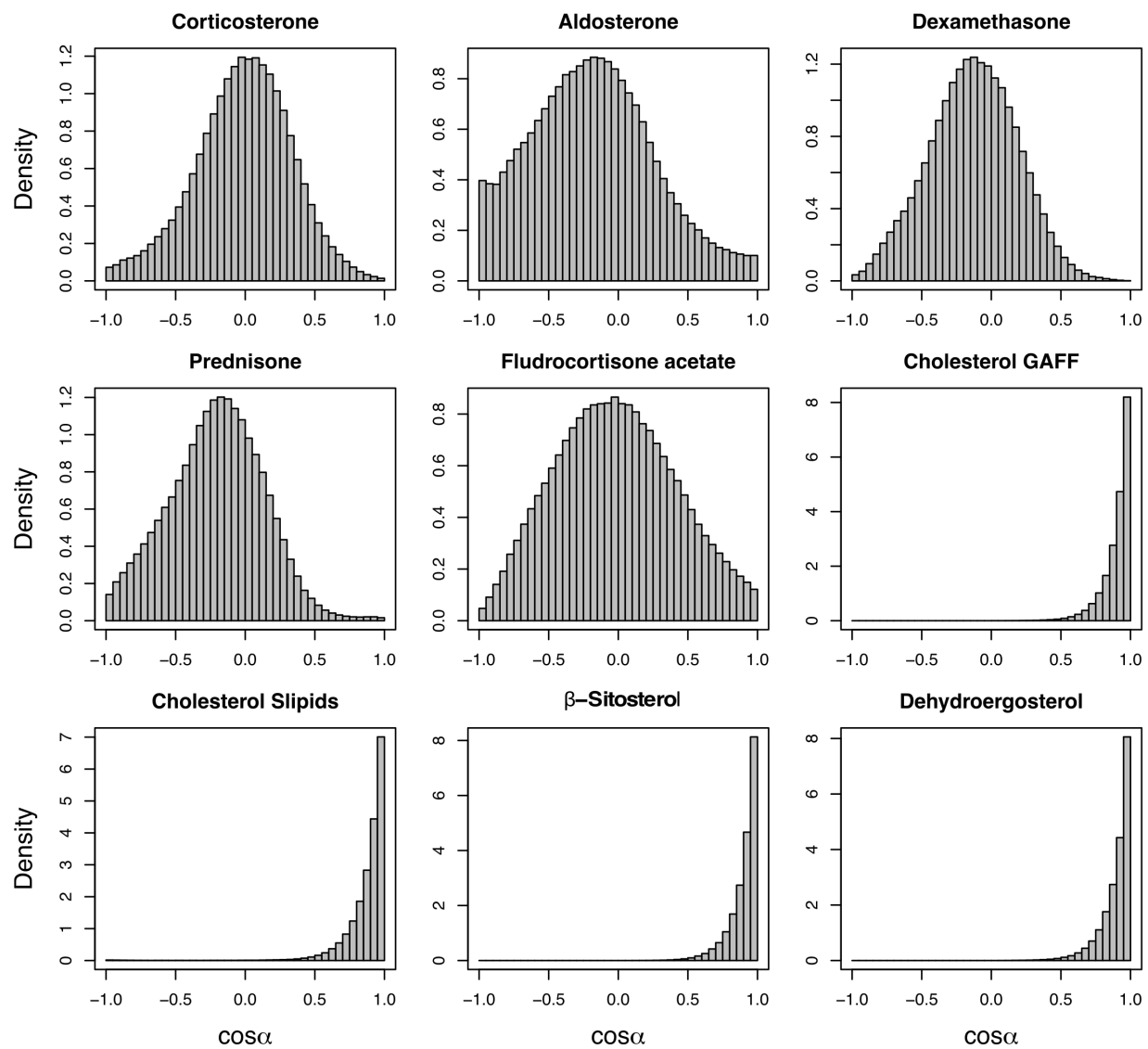


Figure S1 (Cont.): Distributions of the cosine of the tilting angle α of each steroid from 500 ns simulations.

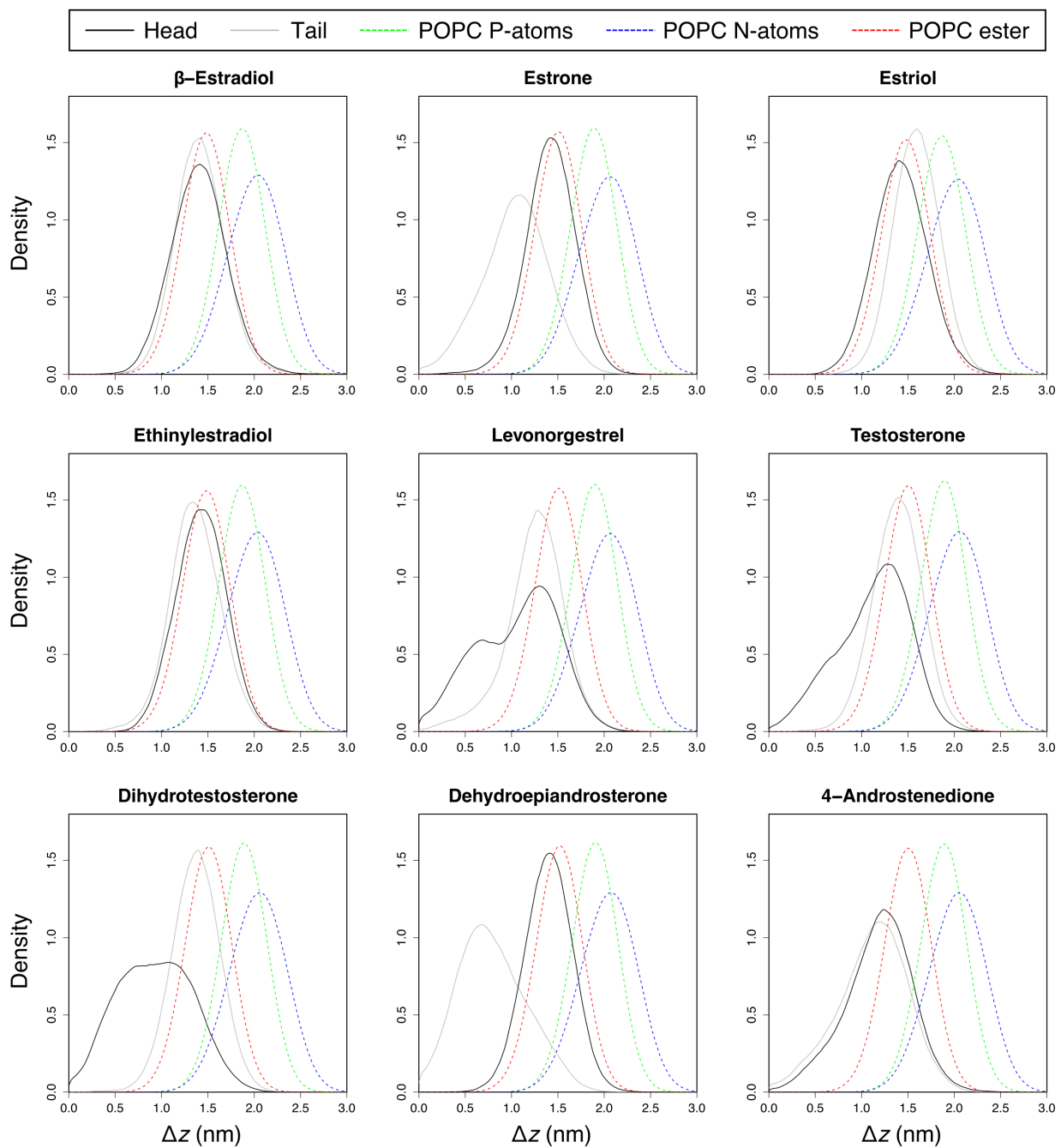


Figure S2: Distributions of the vertical distance z of the head and tail atoms of each steroid from the membrane COM, each computed from 500 ns of simulation. The distributions of the POPC nitrogen, phosphorus, and ester-oxygen atoms are shown in blue, green, and red, respectively.

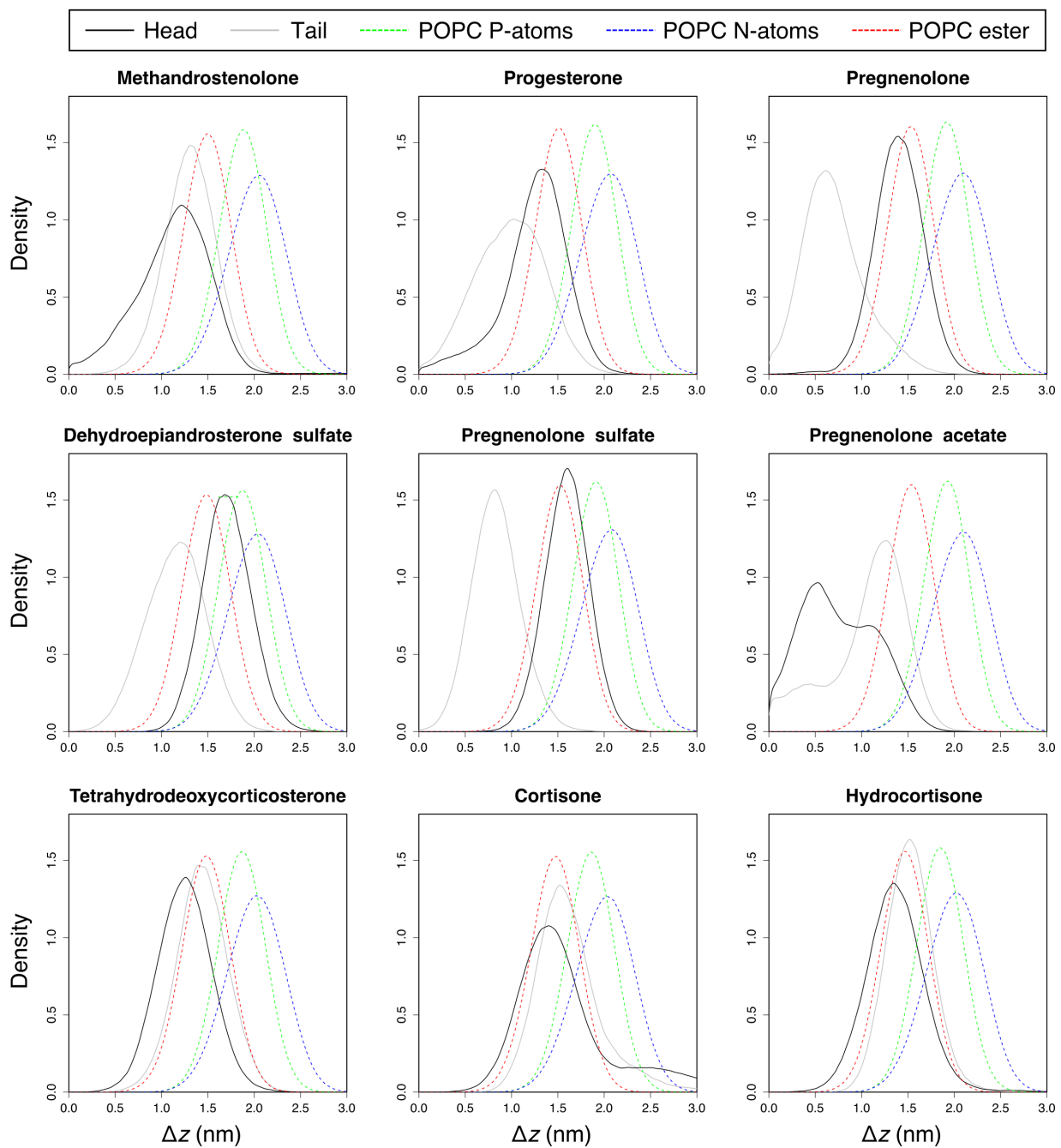


Figure S2 (Cont.): Distributions of the vertical distance z of the head and tail atoms of each steroid from the membrane COM from 500 ns simulations. For orientation, the distributions of the POPC nitrogen, phosphorus, and ester-oxygen atoms are shown in blue, green, and red, respectively.

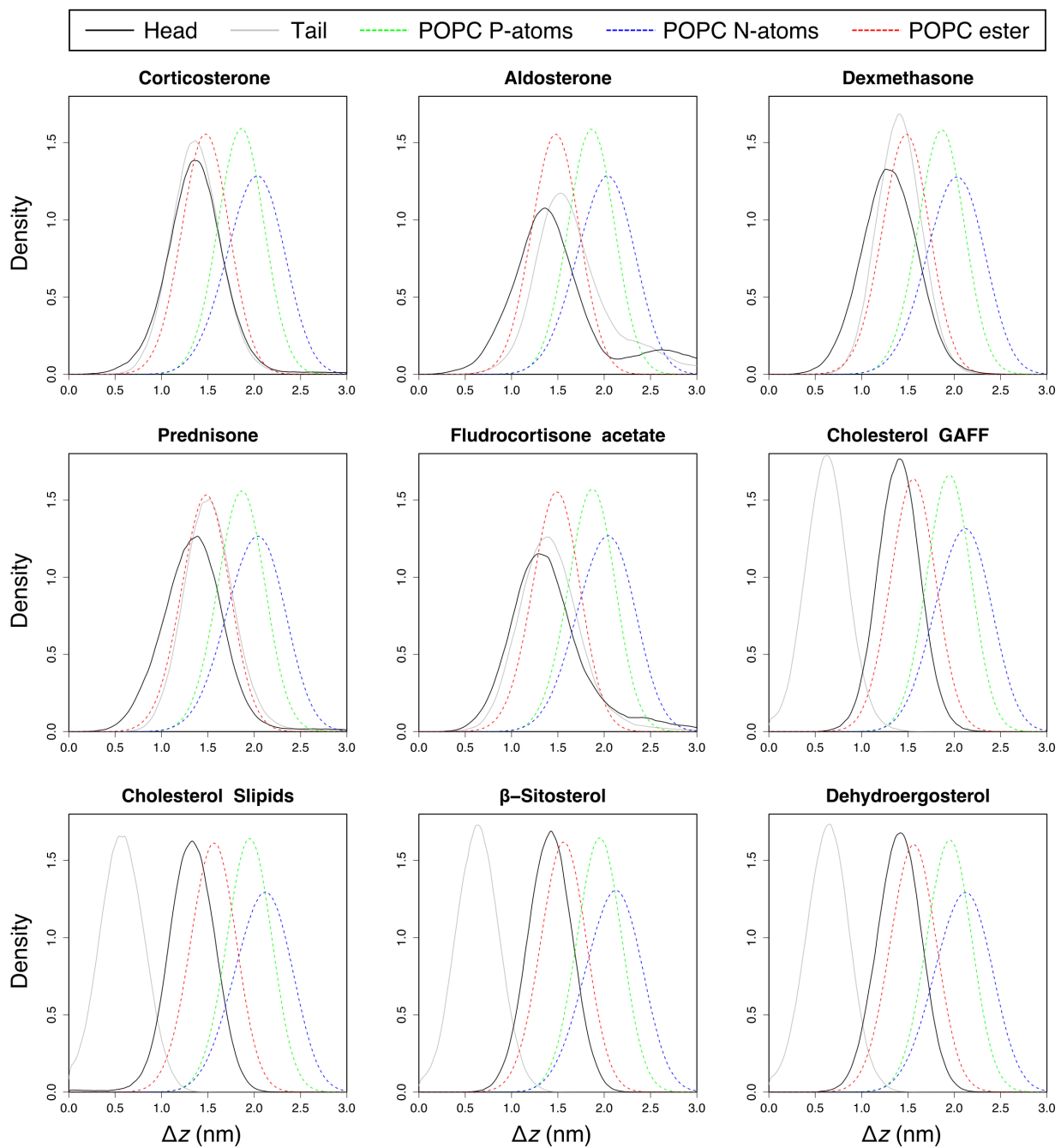


Figure S2 (Cont.): Distributions of the vertical distance z of the head and tail atoms of each steroid from the membrane COM from 500 ns simulations. For orientation, the distributions of the POPC nitrogen, phosphorus, and ester-oxygen atoms are shown in blue, green, and red, respectively.

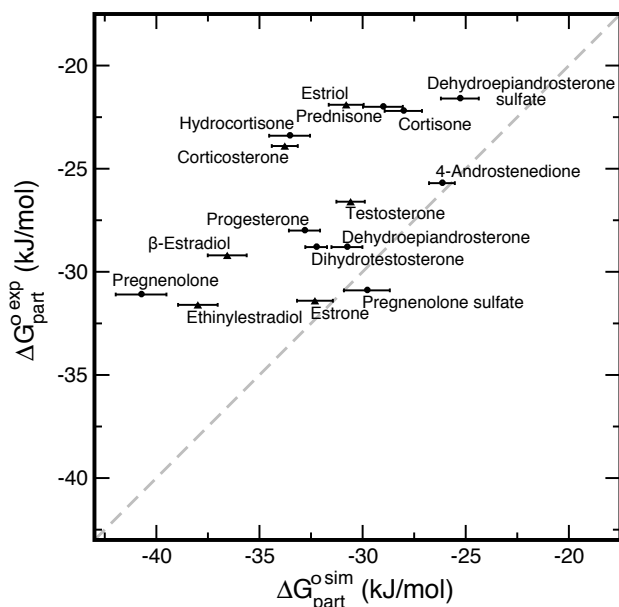


Figure S3: Experimental ($\Delta G_{\text{part}}^{\circ \text{exp}}$) vs. calculated ($\Delta G_{\text{part}}^{\circ \text{sim}}$) free energies of partitioning between water and a POPC bilayer, using partial atomic charges as derived from ESP calculations in vacuum (see Methods). Bars represent calculated standard errors. Experimental standard errors were $\leq 0.5 \text{ kJ mol}^{-1}$ (see Table S1). Experimental values for estrone, β -estradiol, and ethinylestradiol from ref. 27, for estriol from ref. 26, for testosterone from ref. 24, and for corticosterone from ref. 25 (triangles). The rest of the experimental values were obtained by ITC (circles).

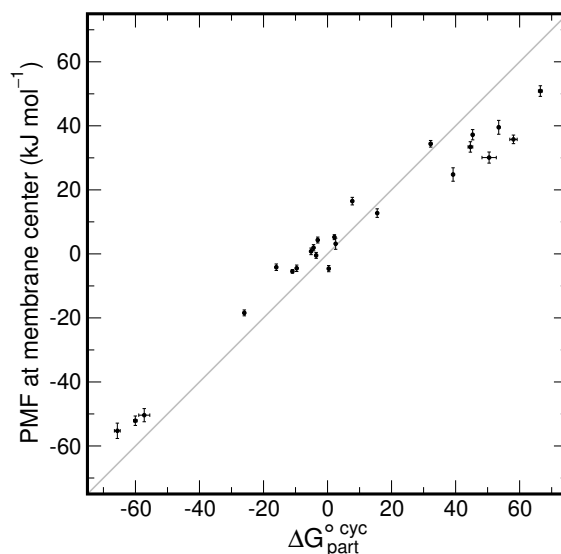


Figure S4: Cyclohexane/water partition free energy ($\Delta G_{\text{part}}^{\circ \text{cyc}}$) versus the free energy for transferring the steroid from bulk to the center of the membrane. The latter was taken from PMFs used for computing the flip-flop rates, evaluated at $z = 0$ (membrane center). Four such PMFs are shown in Fig. 8C. Evidently, $\Delta G_{\text{part}}^{\circ \text{cyc}}$ correlates with the transfer free energy from bulk to the membrane center.

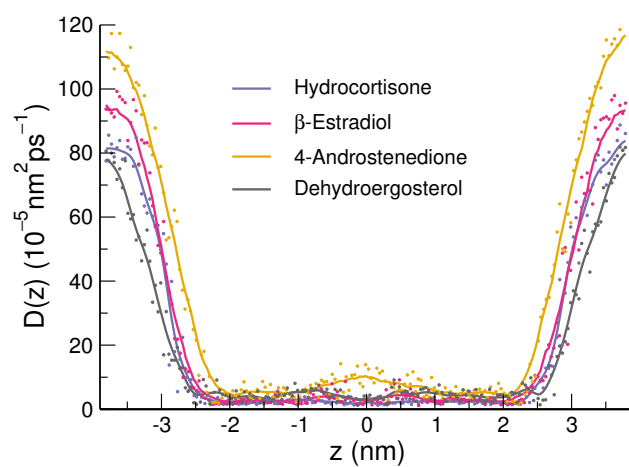


Figure S5: Transversal diffusion coefficients $D(z)$ of four typical steroids as function of position along the membrane normal, see legend for the color code. Dots: values obtained from individual umbrella windows. Lines: smoothed diffusion coefficients. Inside the membrane ($-2 \text{ nm} < z < 2 \text{ nm}$), $D(z)$ varies only moderately between different steroids, suggesting that variations of flip-flop and exit rates are not dominated by variations of $D(z)$ but instead by variations of the PMFs.

Table S1: Thermodynamics of water/membrane partitioning of steroids by ITC. Shown are best-fit values and 95% confidence intervals for the mole-ratio partition coefficient, K_0 (K_{app} for the charged steroids, based on a mole fraction of the steroid in the bilayer of 5.9%), as well as the standard molar quantities of partitioning, namely enthalpy, $\Delta H_{part}^{\circ exp}$, the Gibbs free energy, $\Delta G_{part}^{\circ exp}$, and the entropic contribution, $-T\Delta S_{part}^{\circ exp}$. Several measurements of different lipid concentrations were analyzed globally. Also shown are POPC concentrations in the ITC injection syringe $[POPC]_{syr}$. The concentration of the steroid in the ITC sample cell was 50 μ M for all measurements. If not indicated otherwise, measurements were performed at 27°C, with the effective charge, $z_e = 0$.

Steroid	$[POPC]_{syr}$ (mM)	$K_{0/app}$ (1/mM)	$\Delta H_{part}^{\circ exp}$ (kJ/mol)	$\Delta G_{part}^{\circ exp}$ (kJ/mol)	$-T\Delta S_{part}^{\circ exp}$ (kJ/mol)
4-androstenedione	30/45	0.53 (0.45–0.62)	–7.0 (–8.1–6.0)	–25.7 (–26.1–25.2)	–18.7 (–20.0–17.1)
Cortisone	30/60	0.13 (0.10–0.17)	–15.6 (–22.5–11.6)	–22.2 (–22.8–21.4)	–6.5 (–11.2–1.1)
Dihydrotestosterone	22.5/45	1.83 (1.40–2.38)	–3.9 (–4.6–3.4)	–28.8 (–29.4–28.1)	–24.8 (–26.0–23.5)
Hydrocortisone	60/90	0.21 (0.18–0.25)	–11.6 (–13.7–10.0)	–23.4 (–23.7–22.9)	–11.7 (–13.7–9.3)
Prednisone	30/60/90	0.12 (0.08–0.17)	–12.6 (–21.6–8.3)	–22.0 (–22.9–20.8)	–9.4 (–14.6–0.8)
Dehydroepiandrosterone 22° C	20	2.31 (2.03–2.62)	–15.7 (–17.1–14.5)	–28.8 (–29.2–28.5)	–13.2 (–14.7–11.4)
Dehydroepiandrosterone sulfate 22° C, $z_e = -1$	100	0.12 (0.10–0.15)	–41.4 (–49.5–35.3)	–21.6 (–22.1–21.1)	19.8 13.2–28.4
Pregnenolone 22° C	20/100	5.87 (2.24–27.00)	–1.5 (–1.8–1.3)	–31.1 (–34.9–28.8)	–29.6 (–33.6–27.0)
Pregnenolone sulfate 22° C, $z_e = -1$	20	5.34 (4.70–6.08)	–18.1 (–19.0–17.3)	–30.9 (–31.2–30.6)	–12.8 (–13.9–11.6)
Progesterone 22° C	20/80/80/100	1.64 (1.23–2.19)	–10.1 (–12.1–8.5)	–28.0 (–28.7–27.3)	–17.9 (–20.2–15.2)

References

- (1) Jämbeck, J. P. M.; Lyubartsev, A. P. Derivation and Systematic Validation of a Refined All-Atom Force Field for Phosphatidylcholine Lipids. *J Phys Chem B* **2012**, *116*, 3164–3179.
- (2) Jämbeck, J. P. M.; Lyubartsev, A. P. An Extension and Further Validation of an All-Atomistic Force Field for Biological Membranes. *J Chem Theory Comput* **2012**, *8*, 2938–2948.

- (3) Jämbeck, J. P. M.; Lyubartsev, A. P. Another Piece of the Membrane Puzzle: Extending Slipids Further. *J Chem Theory Comput* **2013**, *9*, 774–784.
- (4) Jorgensen, W. L.; Chandrasekhar, J.; Madura, J. D.; Impey, R. W.; Klein, M. L. Comparison of Simple Potential Functions for Simulating Liquid Water. *J Chem Phys* **1983**, *79*, 926–935.
- (5) Wang, J.; Wang, W.; Kollman, P. A.; Case, D. A. Automatic Atom Type and Bond Type Perception in Molecular Mechanical Calculations. *J Mol Graph Model* **2006**, *25*, 247–260.
- (6) Wang, J.; Wolf, R. M.; Caldwell, J. W.; Kollman, P. A.; Case, D. A. Development and Testing of a General Amber Force Field. *J Comput Chem* **2004**, *25*, 1157–1174.
- (7) Frisch, M. J. et al. Gaussian 09 Revision E.01. 2016; Gaussian Inc. Wallingford CT 2016.
- (8) Sousa da Silva, A. W.; Vranken, W. F. ACPYPE - AnteChamber PYthon Parser InterfacE. *BMC Res Notes* **2012**, *5*, 367.
- (9) Knight, C. J.; Hub, J. S. MemGen: A General Web Server for the Setup of Lipid Membrane Simulation Systems. *Bioinformatics* **2015**, *31*, 2897–2899.
- (10) Pronk, S.; Páll, S.; Schulz, R.; Larsson, P.; Bjelkmar, P.; Apostolov, R.; Shirts, M. R.; Smith, J. C.; Kasson, P. M.; van der Spoel, D.; Hess, B.; Lindahl, E. GROMACS 4.5: A High-Throughput and Highly Parallel Open Source Molecular Simulation Toolkit. *Bioinformatics* **2013**, *29*, 845–854.
- (11) Miyamoto, S.; Kollman, P. A. SETTLE: An Analytical Version of the SHAKE and RATTLE Algorithm for Rigid Water Models. *J Comput Chem* **1992**, *13*, 952–962.
- (12) Hess, B.; Bekker, H.; Berendsen, H. J. C.; Fraaije, J. G. E. M. LINCS: A Linear Constraint Solver for Molecular Simulations. *J Comput Chem* **1997**, *18*, 1463–1472.
- (13) Darden, T.; York, D.; Pedersen, L. Particle Mesh Ewald: An N·log(N) Method for Ewald Sums in Large Systems. *J Chem Phys* **1993**, *98*, 10089–10092.

- (14) Essmann, U.; Perera, L.; Berkowitz, M. L.; Darden, T.; Lee, H.; Pedersen, L. G. A Smooth Particle Mesh Ewald Method. *J Chem Phys* **1995**, *103*, 8577–8593.
- (15) Bussi, G.; Donadio, D.; Parrinello, M. Canonical Sampling Through Velocity Rescaling. *J Chem Phys* **2007**, *126*, 014101.
- (16) Berendsen, H. J. C.; Postma, J. P. M.; van Gunsteren, W. F.; DiNola, A.; Haak, J. R. Molecular Dynamics with Coupling to an External Bath. *J Chem Phys* **1984**, *81*, 3684–3690.
- (17) Klingler, J.; Keller, S. In *Peptide–Membrane Interactions Studied by Isothermal Titration Calorimetry*; Bastos, M., Ed.; CRC Press: Boca Raton, FL, 2016; pp 153–167.
- (18) Keller, S.; Vargas, C.; Zhao, H.; Piszczek, G.; Brautigam, C. A.; Schuck, P. High-Precision Isothermal Titration Calorimetry with Automated Peak-Shape Analysis. *Analytical chemistry* **2012**, *84*, 5066–5073.
- (19) Vargas, C.; Klingler, J.; Keller, S. Membrane Partitioning and Translocation Studied by Isothermal Titration Calorimetry. *Membrane Biogenesis: Methods and Protocols* **2013**, 253–271.
- (20) Tsamaloukas, A. D.; Keller, S.; Heerklotz, H. Uptake and Release Protocol for Assessing Membrane Binding and Permeation by Way of Isothermal Titration Calorimetry. *Nat Protoc* **2007**, *2*, 695–704.
- (21) Kemmer, G.; Keller, S. Nonlinear Least-Squares Data Fitting in Excel Spreadsheets. *Nat Protoc* **2010**, *5*, 267–281.
- (22) Keller, S.; Heerklotz, H.; Blume, A. Monitoring Lipid Membrane Translocation of Sodium Dodecyl Sulfate by Isothermal Titration Calorimetry. *J Am Chem Soc* **2006**, *128*, 1279–1286.
- (23) Keller, S.; Böthe, M.; Bienert, M.; Dathe, M.; Blume, A. A Simple Fluorescence-Spectroscopic Membrane Translocation Assay. *ChemBioChem* **2007**, *8*, 546–552.

- (24) Tipping, E.; Ketterer, B.; Christodoulides, L. Interactions of Small Molecules with Phospholipid Bilayers. Binding to Egg Phosphatidylcholine of Some Uncharged Molecules (2-Acetylaminofluorene, 4-Dimethylaminoazobenzene, Oestrone and Testosterone) That Bind to Ligandin and Aminoazo-Dye-Binding Protein A. *Biochem J* **1979**, *180*, 319–326.
- (25) Golden, G.; Rubin, R.; Mason, R. Steroid Hormones Partition to Distinct Sites in a Model Membrane Bilayer: Direct Demonstration by Small-Angle X-Ray Diffraction. *Biochimica et Biophysica Acta (BBA)-Biomembranes* **1998**, *1368*, 161–166.
- (26) Yamamoto, H.; Liljestrand, H. M. Partitioning of Selected Estrogenic Compounds Between Synthetic Membrane Vesicles and Water: Effects of Lipid Components. *Environ Sci Technol* **2004**, *38*, 1139–1147.
- (27) Kwon, J.-H.; Liljestrand, H. M.; Katz, L. E.; Yamamoto, H. Partitioning Thermodynamics of Selected Endocrine Disruptors Between Water and Synthetic Membrane Vesicles: Effects of Membrane Compositions. *Environ Sci Technol* **2007**, *41*, 4011–4018.
- (28) Kirkwood, J. G. Statistical Mechanics of Fluid Mixtures. *J Chem Phys* **1935**, *3*, 300–313.
- (29) Torrie, G. M.; Valleau, J. P. Monte Carlo Free Energy Estimates Using Non-Boltzmann Sampling: Application to the Sub-Critical Lennard-Jones Fluid. *Chem Phys Lett* **1974**, *28*, 578–581.
- (30) Nitschke, N.; Atkovska, K.; Hub, J. S. Accelerating Potential of Mean Force Calculations for Lipid Membrane Permeation: System Size, Reaction Coordinate, Solute-Solute Distance, and Cutoffs. *J Chem Phys* **2016**, *145*, 125101.
- (31) Zoicher, F.; van der Spoel, D.; Pohl, P.; Hub, J. S. Local Partition Coefficients Govern Solute Permeability of Cholesterol-Containing Membranes. *Biophys J* **2013**, *105*, 2760–2770.
- (32) Van Gunsteren, W. F.; Berendsen, H. J. C. A Leap-Frog Algorithm for Stochastic Dynamics. *Mol Simul* **1988**, *1*, 173–185.

- (33) Kumar, S.; Rosenberg, J. M.; Bouzida, D.; Swendsen, R. H.; Kollman, P. A. The Weighted Histogram Analysis Method for Free-Energy Calculations on Biomolecules. I. The Method. *J Comput Chem* **1992**, *13*, 1011–1021.
- (34) Hub, J. S.; Winkler, F. K.; Merrick, M.; de Groot, B. L. Potentials of Mean Force and Permeabilities for Carbon Dioxide, Ammonia, and Water Flux Across a Rhesus Protein Channel and Lipid Membranes. *J Am Chem Soc* **2010**, *132*, 13251–13263.
- (35) van der Spoel, D.; van Maaren, P. J.; Caleman, C. GROMACS Molecule & Liquid Database. *Bioinformatics* **2012**, *28*, 752–753.
- (36) Bennett, W. F. D.; MacCallum, J. L.; Hinner, M. J.; Marrink, S. J.; Tieleman, D. P. Molecular View of Cholesterol Flip-Flop and Chemical Potential in Different Membrane Environments. *J Am Chem Soc* **2009**, *131*, 12714–12720.
- (37) Jo, S.; Rui, H.; Lim, J. B.; Klauda, J. B.; Im, W. Cholesterol Flip-Flop: Insights from Free Energy Simulation Studies. *J. Phys. Chem. B* **2010**, *114*, 13342–13348.
- (38) Parisio, G.; Sperotto, M. M.; Ferrarini, A. Flip-Flop of Steroids in Phospholipid Bilayers: Effects of the Chemical Structure on Transbilayer Diffusion. *J. Am. Chem. Soc.* **2012**, *134*, 12198–12208.
- (39) Neale, C.; Madill, C.; Rauscher, S.; Pomès, R. Accelerating Convergence in Molecular Dynamics Simulations of Solutes in Lipid Membranes by Conducting a Random Walk Along the Bilayer Normal. *J. Chem. Theory Comput.* **2013**, *9*, 3686–3703.
- (40) Weinan, E.; Ren, W.; Vanden-Eijnden, E. String Method for the Study of Rare Events. *Phys. Rev. B* **2002**, *66*, 052301.
- (41) Hummer, G. Position-Dependent Diffusion Coefficients and Free Energies from Bayesian Analysis of Equilibrium and Replica Molecular Dynamics Simulations. *New J. Phys.* **2005**, *7*, 34.

- (42) Endress, E.; Heller, H.; Casalta, H.; Brown, M. F.; Bayerl, T. M. Anisotropic Motion and Molecular Dynamics of Cholesterol, Lanosterol, and Ergosterol in Lecithin Bilayers Studied by Quasi-Elastic Neutron Scattering. *Biochemistry* **2002**, *41*, 13078–13086.
- (43) Hänggi, P.; Talkner, P.; Borkovec, M. Reaction-Rate Theory: Fifty Years After Kramers. *Rev. Mod. Phys.* **1990**, *62*, 251.
- (44) Pohl, P.; Saparov, S. M.; Antonenko, Y. N. The Size of the Unstirred Layer As a Function of the Solute Diffusion Coefficient. *Biophys. J.* **1998**, *75*, 1403–1409.
- (45) Xiang, T.-X.; Anderson, B. D. Development of a Combined NMR Paramagnetic Ion-Induced Line-Broadening/dynamic Light Scattering Method for Permeability Measurements Across Lipid Bilayer Membranes. *J. Pharm. Sci.* **1995**, *84*, 1308–1315.
- (46) Seki, T.; Mochida, J.; Okamoto, M.; Hosoya, O.; Juni, K.; Morimoto, K. Measurement of Diffusion Coefficients of Parabens and Steroids in Water and 1-Octanol. *Chem. Pharm. Bull.* **2003**, *51*, 734–736.